Fabrication and Evaluation of Polycaprolactone Beads-on-string Membranes for Applications in Bone Tissue Regeneration

Jaime Santillán[1,5], Emmanuel A. Dwomoh[2], Yaiel G. Rodríguez-Avilés[3], Samir A. Bello[3], and Eduardo Nicolau[4,5*]

[1] *Department of Physics, University of Puerto Rico, Rio Piedras Campus, 17 Ave. Universidad Ste. 1701, San Juan, Puerto Rico USA 00925-2537*

[2] *Department of Biology, City University of New York, City College, New York, NY 10031, USA*

[3] *Department of Biology, University of Puerto Rico, Rio Piedras Campus, 17 Ave. Universidad Ste. 1701, San Juan, Puerto Rico USA 00925-2537*

[4] *Department of Chemistry, University of Puerto Rico, Rio Piedras Campus, 17 Ave. Universidad Ste. 1701, San Juan, Puerto Rico USA 00925-2537*

[5]*Molecular Science Research Center, University of Puerto Rico, 1390 Ponce De León Ave, Suite 2, San Juan Puerto Rico USA 00931-3346*

*Corresponding author: Eduardo Nicolau
Phone: 787-292-9820, fax: 787-522-2150; email: eduardo.nicolau@upr.edu

KEYWORDS polycaprolactone, electrospinning, beads-on-string, scaffold, bone tissue regeneration

ABSTRACT

Tissue engineering leads the development of biomaterial scaffolds where its biocompatibility and bioactivity is often improved after performing physical or chemical surface modification treatments. Micropatterning, soft lithography, and biofabrication are also approaches that provide a biomimetic microenvironment but have proven very costly and time-consuming. In this concern, an appropriate substrate with suitable sites for cell attachment represents a major factor in cell behavior and biological functions. For this reason, our strategy was to fabricate a standard fibrous biomaterial with reproducible surface topography, incorporating microbeads and nanofeatures, and show the positive outcomes of the new substrate reflected on cell functions of bone cells. The electrospun PCL beads-on-string membranes were obtained adjusting the spinning solution at different concentrations until continuous beads were formed. Cell adhesion and proliferation, on the PCL scaffold, were analyzed the subsequent 2 days after initial culture. Complementary studies of cytoskeleton spreading, and differentiation were analyzed after 7 and 14 days of the initial incubation. The Scanning Electron Microscopy (SEM) images showed evidence of the formation beads-on-string nanofibers and suggested that as-formed microstructures worked as attachment sites for osteoblasts. We investigated cell proliferation using anti-BrdU fluorescence assay and results show a similar proliferation rate of cells cultured between PCL scaffolds and control. Finally, Phalloidin TRITC and anti-sialoprotein antibody were used to analyze cell spreading and differentiation after 7 and 14 days, respectively. This work shows a low-cost fabrication method to produce a biodegradable scaffold with micro/nanostructured characteristics that favor cell adhesion, proliferation, maturation and subsequent differentiation of osteoblasts. According to the results, biocompatibility of PCL

beads-on-string could be comparable to other complex biomaterials and we conclude that our scaffold is optimal for applications in bone tissue regeneration.

1. INTRODUCTION

The intrinsic hierarchical configuration of the extracellular matrix (ECM), is composed by a dynamic network of macromolecules that serves as structural support as well as its molecular components are capable to activate biochemical and biophysical cues that regulate cell morphology, proliferation, and tissue formation [1-2]. In recent years, new approaches combining nanotechnology and synthetic biomaterials, have resulted in fabrication of state-of-the-art scaffolds that closely mimic both the geometry of the matrix [3] and regulatory characteristics of native-like ECM [4-5]. The high incidence of disorders and conditions related to bone diseases [6] have motivated the rapid progress of polymeric biomaterials focused on bone tissue regeneration (BTR). Innovation and new perspectives of BTR have made it a promising field of biomedical research [7-8].

Polymeric biomaterials have been extensively studied in the investigation and fabrication of scaffolds that allow the regeneration of diverse types of tissues including tendons [9], ligaments [10], bone [11], blood vessels [12] etc. TE combines strategically cells, scaffolds and biochemical factors pursuing the target of replacing or regenerate physiological function of tissues and organs. Otherwise, the application of nanotechnology has boosted the scaffold research and has developed novel nanostructured biomaterials for bone tissue regeneration [13]. Those nanostructured bone scaffolds allow resembling the micro and nanoscale environment of self-assembling collagen fibers, elastic fibers and protein-polysaccharides, mostly found in mammals ECM and fibrous tissues [14-15]. Two strategies, commonly used, to improve the biocompatibility

of polymeric scaffolds are the modification of surface properties through physicochemical/biological methods and the designing of engineered surface topography, frequently employed for tailoring biomedical applications [16]. In addition to the latter, the acquired surface characteristics also promote better cell attachment, boost cell proliferation, and stimulate differentiation of osteoblastic cells [17]. The surface modification methods are used to improve surface properties of polymer scaffolds. These typical treatments include dry plasma [18], wet chemistry [19], UV [20], gamma radiation [21], subsequently involves additional processing steps, as well as costly and high-tech equipment that could be considered limiting factors. However, to elucidate the influence of topographical features of scaffolds in osteoblastic functions, our work provides a feasible, reproducible and low-cost technology with the ability to recreate the similar micro and nanoscale structures of the bone matrix, and led to enhance the grip between the growing bone tissue and the scaffold [22-23].

In this framework, electrospinning technique arises as the most effective, versatile and inexpensive tool for fabrication of engineered fibrous scaffold using biopolymers [24-25]. Polymeric nanofibers with controlled morphologies and diameter of fibers, called beads-on-string, are considered a safe and non-invasive approach to modulate cellular response because their surface topography could be addressed only adjusting working parameters of electrospinning[26-29]. Further, electrospun nanofibers offer other several advantages for bone tissue regeneration such as, formation of a highly porous membrane that works as interconnected microchannel network for mass transport likewise better cell infiltration and possible future neovascularization, a fibrous micro and nanostructured topography that mimic a 3D *in vivo* environment that could influence osteoblasts phenotype, and finally, a high surface-area that provide additional adsorption sites for bioactive molecules that improve cell attachment [30-32].

During past years, the presence of beads in nanofibers, formed during the electrospinning process, were considered undesired defects because they reduce the uniformity of nanofibers. Beaded fibers formed during electrospinning are often considered by-products by researchers and are avoided optimizing the solution parameters, such as the concentration of the polymer solution and the viscosity [28, 33]. For instance, at a lower polymeric concentration a mixture of beads and fibers, a beads-on-string like structure, is formed. The surface tension and surface charge density are also considered main factors contributing on the control of nanofibers morphology, thus when it overcomes viscosity of the solution, it favors formations of beaded fibers that exhibit a greater surface area for cell growth[29].

Recently, aliphatic polyester-based polymers including polycaprolactone (PCL) [34-35], poly (3-hydroxy valerate) [36], polylactic acid (PLA) [37], polyhydroxy butyrate (PHB) [38], and polyglycolic acid (PGA) [39] are receiving special attention for use on TE, because of their biodegradability, predictable degradation rate and biocompatibility. Among of them, PCL is a synthetic polymer approved for the Food and Drug Administration (FDA) and has been intensively studied to be implanted in the human body. Currently, PCL is used in TE, medical and surgical applications such as drug delivery systems, implantable biomaterials, packaging materials, absorbable sutures and in contraceptive devices [40-41]. Furthermore, PCL is strongly hydrophobic, possess a semi-crystalline microstructure which extends its resorption time, desirable mechanical properties, and degradation by hydrolytic mechanisms in a controller manner under physiological environment [42-43]. The latter properties make PCL an ideal biopolymer for long-term implant devices as well as a good candidate to load-bearing applications, and support tissues with limited capacity to repair itself such as bone, cartilage, ligaments, and dental structures [44].

Several studies have reported, separately, the application of beads and nanofibers as scaffolds that support cell growth [45-47]. Recently, Rinoldi et al. (2018) demonstrated that the topography and the presence of beads and fibrous structures enhance cell adhesion and proliferation, making this beaded scaffold suitable for tendon regeneration [48]. However, to our knowledge, there have been no studies that joined efforts to address both approaches together for BTR.

Consequently, in the present work, we produce electrospun beads-on-string scaffolds where its hierarchical topography produces a positive effect [48-49], that influences the osteoblasts functions as adhesion, proliferation, and differentiation. Finally, we propose PCL beads-on-string scaffolds as an alternative approach for bone tissue regeneration.

2. MATERIAL AND METHODS

2.1. Materials

All reagents used in this work were analytical reagent grade and no additional purification process was required. Polycaprolactone pellets with an average molecular weight of 80,000, was purchased from Sigma Aldrich (USA). N, N-Dimethylformamide (DMF) was purchased from Fisher Scientific (USA) and it was used as a solvent for PCL. Human fetal osteoblastic cells hFOB 1.19 (ATCC® CRL-11372™) were used to examine the effect of beads on cell behavior.

2.2. Preparation of PCL beads-on-string scaffolds

A polymer solution of 14% w/v was prepared by dissolving PCL pellets in DMF solvent. For a complete dispersion, the PCL/DMF solution was magnetically stirred at 110˚C for ~2 hours. Horizontal electrospinning setup and a rotating drum collector was used in this work. As the first step of the electrospinning process, 3mL of the polymer solution was placed into a disposable syringe and dispensed through a metallic 22-gauge needle. In this study, PCL/DMF

solution was infused at a constant rate (0.4mL/h) and regulated by a basic syringe pump (NE-300 Just Infusion™). Finally, The PCL/DMF solution was electrospun applying a high DC voltage (Gamma High Voltage Research, Florida, USA) in the range of 10KV to 20KV. The randomly-oriented beaded nanofibers were deposited on the rotating collector until they form the desired membrane. The electrospinning procedure was performed at room temperature of 75˚F ± 5 and at a humidity of 86 % ± 5. A fixed distance of 10 cm was placed between the steel needle and the rotating collector. After the electrospinning process, the membranes were soaked in nanopure water for 3 days, then soaked overnight with 70% ethanol followed by UV radiation before cell culture. In addition, the design matrix of the experiment was shown in **Supporting Information Table S1** and SEM results were shown in **Figure S1.**

2.3. Characterization of electrospun beads-on-string membranes

Characterization of beads-on-string membranes was performed using physical and chemical surface analysis techniques

2.3.1. Scanning Electron Microscopy (SEM)

Morphology and diameter of the beaded nanofibers were investigated and characterized by scanning electron microscopy (SEM) (JEOL JSM-7500F and JEOL 6480LV, high vacuum mode, 20 kV). To improve the imaging of samples analyzed by SEM, each sample was mounted on an aluminum stage and then was sputtered with 10 nm of gold prior to SEM imaging. We selected a region of a PCL membrane to obtain an average diameter of beads and nanofibers using ImageJ, a software developed at NIH.

2.3.2. Atomic Force Microscopy (AFM)

Morphological characterization of PCL nanofibers was visualized by an atomic force AFM Bruker multimode 8. The topography of nanofibers was visualized by Tapping Mode in ambient conditions. Silicon AFM probe with a spring constant of 40 N/m was used to scan the fiber surface at a resonance frequency of 400KHz. Then, analysis of the AFM images was conducted to using Nanoscope Analysis software.

2.3.3. X-Ray Diffraction (XRD)

A Rigaku SmartLab X-Ray diffractometer was used for diffraction measurements of the PCL membranes. X-Ray spectrum was performed using a Cu radiation with recommended operating conditions of 40KV and a 44mA. It uses a goniometer with scattering angles (2θ) that varied from 10° to 40° at a scan speed of 3.0°/min.

2.3.4. Fourier-transform infrared spectroscopy (FTIR)

An attenuated total reflectance Fourier-transform infrared spectrometer (Bruker Tensor 27) was used to determine the functional groups present in the PCL pellets and the electrospun PCL beaded membranes. Air was used as a blank control over the same wavenumber range where the samples were analyzed. All spectra were obtained between 4000 and 500 cm^{-1} and the number of scans was fixed to 64 with a resolution of 4 cm^{-1}.

2.3.5. Mechanical properties

CT3 Texture Analyzer (Brookfield Engineering, USA) was used to conduct uniaxial tensile testing of PCL membranes at ambient conditions. Samples were sectioned into rectangular strips measuring 14 mm in width and 16 mm in length and 0.4 mm of thickness. Specimens were loaded to failure at a strain rate of 0.5 mm/s. The measurements and analysis of

the strain-stress curve were performed using OriginPro 9.0 software. The linear section of the graph was used to determine the modulus of elasticity of the PCL scaffold. At the limit of the elastic region, the yield strength was found and finally, in the plastic region, the ultimate tensile strength (UTS), the fracture point and elongation at break of the biomaterial were obtained. Each measurement was analyzed in triplicate.

2.4. Characterization of surface biocompatibility

Characterization of surface biocompatibility was performed using *in vitro* cell culture and immunocytochemistry assays.

2.4.1. In Vitro Cell Culture

hFOB 1.19 (ATCC® CRL-11372™) cell line was cultured as described in Vega-Figueroa et.al (2017) [50]. Briefly, cells have a doubling time of 36 hours and were subcultured when confluency reached approximately 70% to 80%. In case of cells were not confluent, the culture medium was changed to replenish nutrients. The recommended passage number for this cell line is 4 and were used for the adhesion, proliferation and differentiation assays.

2.4.2. Cell Proliferation

hFOB cells were seeded on PCL scaffolds and glass coverslips (control) placed in 24-well ultralow attachment surface tissue culture plate at a density of 5.0 x10^4 cells/well. Then, the cells were placed in the incubator at least 48 hours before the incorporation of BrdU. Culture media of each well was replaced with 10 μM of bromodeoxyuridine labeling solution (BrdU, Sigma-Aldrich, USA) and incubated for at least 6 hours. Subsequently, a chemical fixation of cells was performed with 4% paraformaldehyde (PFA) for 15 min. After fixation, cells were gently washed three times with Phosphate-Buffered Saline (PBS)(1mL/well), for 5 min each. Cells were permeabilized with 0.1% Triton-100X for 15 min and then carefully rinsed with PBS.

For complete removal of all the permeabilization solution, this rinsing process was repeated three times with 1mL of PBS. Later, cells were incubated with 0.05N HCl for 1 hour. After rinsing with PBS for 5 minutes, the cells were blocked with goat serum (2%, Sigma-Aldrich, USA) for 1h at room temperature to prevent or minimize the non-specific binding of the primary antibody on the substrate surface. Samples were incubated with the monoclonal anti-BrdU mouse antibody (1:5, GE Healthcare) overnight at 4˚C. Next, samples were rinsed with PBS (3x) and incubated with the polyclonal secondary antibody Alexa Fluor 594 AffiniPure Goat Anti-Mouse (1:250, Jackson Immuno Research) for 1 hour. Lastly, after washing the samples with PBS (3x), were mounted on coverslips as described in Vega-Figueroa et.al.[50]

2.4.3. Morphological Study of hFOB Cells by SEM

We used scanning electron microscopy (SEM) to assess the cell morphology and confluence of hFOB cells grown (5.0 x10^4 cells/well) on PCL beads-on-string scaffolds and glass coverslips (control). At 48 hours, 7 and 14 days of cell growth, osteoblastic cells fixed by 4% glutaraldehyde (Sigma-Aldrich, USA) were stored at 4°C overnight. The next day, the glutaraldehyde solution was removed, and fixed cells were rinsed thoroughly (3x) in PBS with intervals of 10 min per rinse. Following this step, dehydration of samples was performed using graded ethanol (10–100%) for 10 min each. Subsequently, the samples were dried in a series of hexamethyldisilane **(**HMDS) (Sigma-Aldrich, USA)/100% ethanol solutions of different ratios for 10 min each: 1:3 HDMS/EtOH100%, 1:1 HDMS/EtOH100% and 3:1 HDMS/EtOH100%. Lastly, cells were washed with 100% HDMS and this process was repeated three times for 10 min each. Next, samples were immersed in 2 mL of pure HMDS, which was left to evaporate overnight. The samples were then mounted on 12.2 mm aluminum mount holder (Ted Pella, Inc.) with adhesive carbon tape and coated with gold (approx. 15 nm). Finally, all the specimens were

imaged using JEOL 6480LV and JEOL JSM-7500F scanning electron microscope under high vacuum mode operating at a voltage of 20 kV.

2.4.4. Cell Morphology and differentiation using Phalloidin and Bone Sialoprotein

In order to evaluate the osteoblast differentiation, bone sialoprotein expression was studied at 7 and 14 days of cell growth on the PCL beads-on-string membrane. 4% paraformaldehyde in PBS is a standard solution used for fixation of cells. After 15 min of fixation at ambient conditions, cells were rinsed three times with PBS and subsequently permeabilized with Triton-100X (0.1% in PBS). After 15 min of permeabilization, cells were rinsed again with PBS. Non-specific sites were blocked by adding 2% goat serum for 1 h. The cells were incubated with anti-bone sialoprotein antibody (1:100, Abcam) and stored at 4˚C overnight. Next day, after three, 10 min washes with PBS, cells were incubated with Phalloidin TRITC (1:250, Sigma Aldrich) mixed for 1 hour with the polyclonal secondary antibody, Alexa Fluor 488 AffiniPure Goat Anti-Rabbit IgG (H+L) (1:250, Jackson Immuno Research). Subsequently, the samples were washed again three times with PBS for 10 min before being mounted on 24 × 60 mm coverslips with ProLong Diamond Antifade reagent containing 4', 6-diamidino-2-phenylindole (DAPI) and stored at room temperature in the dark. Samples were observed and analyzed using a Nikon Eclipse Ni fluorescence microscope with a Nikon DS-Q12 digital camera.

2.4.5 Statistical Analysis

Cell nuclei were counted using CellProfiler software. A software GraphPad Prism 7.0 was used to analyze all subsequent data. Unpaired t-test was used to determine statistical significance, where *** $p < 0.001$; * $p < 0.033$. Data are presented as mean ± standard deviation.

3. RESULTS AND DISCUSSION

3.1. Characterization of the PCL beads-on-string membrane scaffolds

3.1.1. Morphological analysis of fibers by SEM and AFM

Randomly oriented PCL beaded nanofibers were prepared through electrospinning technique at 14% w/v concentration **(Figure 1A)**. In our results, SEM micrographs showed the formation of membranes with microstructures and random-oriented fibers at the nanoscale. The average diameter of beads and nanofibers were found to be 6.52 ± 1.24 microns and 703.25 ± 131.42 nm, respectively **(Figure 1B).** The accomplished scaffold then was used as a scaffold for osteoblastic cells. Representation of cell-seeding on PCL beads-on-string scaffolds is shown in **Figure 1C.**

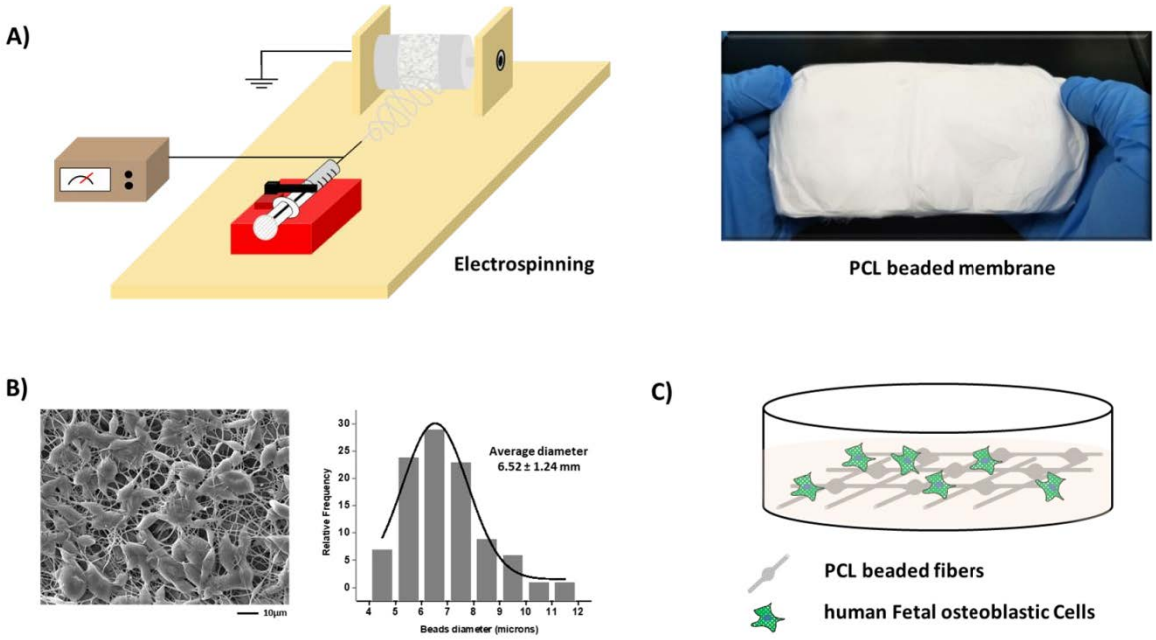

Figure 1. Preparation of PCL scaffolds with nano and micro features. **A)** Schematic for electrospinning system that shows the main components of the experiment: Power supply, syringe pump and rotating collector. Photo image of the obtained PCL beaded membrane **B)** SEM Micrograph and diameter distribution of the PCL beads and nanofibers **C)** Schematic representation of cell culture of hFOB 1.19 cells on PCL beaded nanofibers.

SEM and AFM 3D image show the morphology and topography, respectively of a group of nanofibers as well as further analysis shows that the fiber diameter is around 795 nm (**Figure 2, Supporting Information Figure S2).** These results confirm our membrane provide micro-beads and nano-fibers that could work as cell scaffold, due to its similar hierarchical micro/nanostructured interface found on natural ECM.

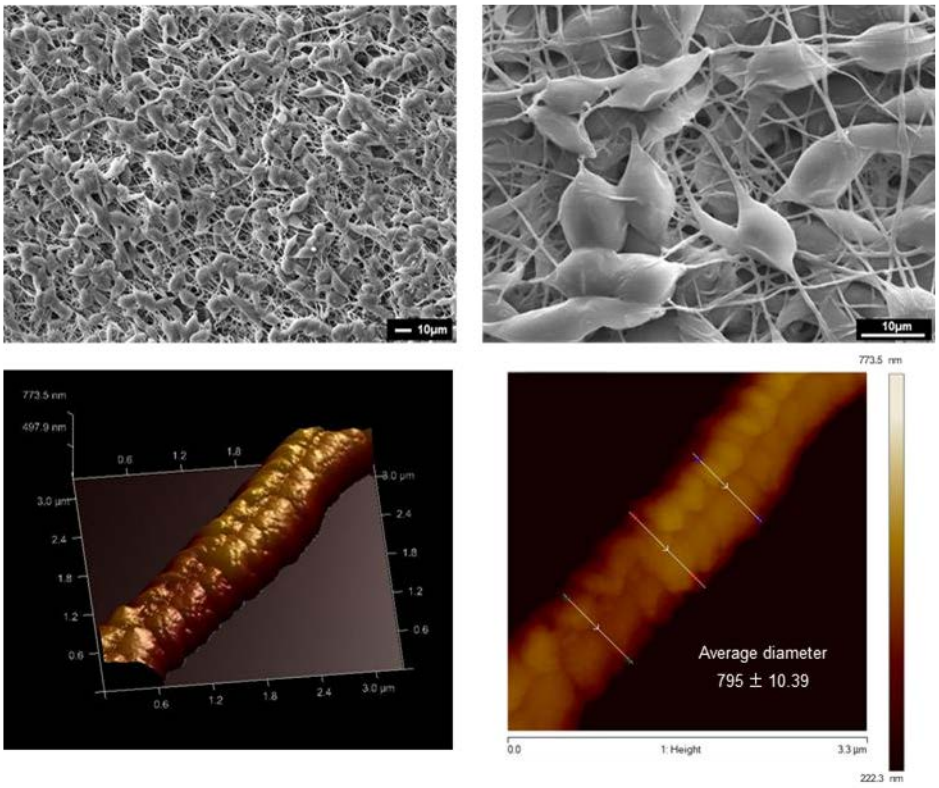

Figure 2. Physical characterization of PCL beads-on-string scaffolds. SEM micrographs show the morphology of the electrospun PCL beads-on-string membrane at different magnifications 500x and 2000x. AFM images of individual electrospun PCL nanofiber. 3D representation of a single nanofiber with an average diameter of nanofiber around 681 ± 75 nm.

3.1.3. FTIR Analysis

Fourier transform infrared spectroscopy (FTIR) was used to identify the chemical composition of the PCL membranes. The FTIR spectra show in **Supporting Information**

Figure S3A peaks bands that allow identifying the functional groups present on PCL pellets and electrospun PCL membranes. The spectrum of PCL displays two characteristics peaks at 2943 cm^{-1} and 2866 cm^{-1}, corresponding to the asymmetric and symmetric stretching vibrational mode of CH_2, respectively. Moreover, an intense and sharp peak at 1722 cm^{-1}, indicates the presence of a carbonyl group, that correspond to the C=O stretching vibration[51]. Additionally, some transmittance peaks between 1500 cm^{-1} and 500 cm^{-1} were also identified as typical peaks present on PCL and are visible around 1293 cm^{-1} corresponding to C-O and C-C stretching, at 1239 cm^{-1} related to asymmetric C-O-C stretching and around 1163 cm^{-1} corresponding to symmetric C-O-C stretching. Interpretation of the obtained FTIR spectra of the raw material and electrospun PCL membranes are found in agreement with previous publications[52-55].

3.1.2. XRD Analysis

X-Ray diffraction analysis was carried out to explore crystallinity of the electrospun PCL membrane. PCL has been broadly used in tissue engineering[56-57] due to it's low *in vivo* degradation rate that is determined by the degree of crystallinity of the polymer [44, 58]. **Supporting Information Figure S2B** shows X-ray diffraction patterns of electrospun PCL membrane and exhibit two characteristics diffraction peaks [52, 59-60] at the Bragg angle 21.2° and at 23.5°, corresponding to the crystal lattice plane (100) and (200), respectively[55, 61]. Finally, the presence of the strong sharp peak confirmed that PCL is a semi-crystalline polymer and also indicates that preserves its structure after the electrospinning process.

3.1.4. Mechanical Properties

Mechanical properties of PCL scaffolds are an important characteristic because the material should mimic the function of native ECM and comparable mechanical properties are

desired. In this concern, PCL beaded membranes must provide support and structural stability for the growth of new cells and future regenerated tissue. The mechanical response under uniaxial stress of PCL membranes strips is shown in **Figure 3A**. PCL specimens were tested under dry conditions at a speed of 0.5 mm/s in a tensile mode and withstand stresses of up to 0.54±0.07 MPa (UTS). The stress-strain curve for PCL membranes shows an elastic region with Young's modulus of 2.29±0.13 MPa and a fracture point of 0.52±0.08MPa. The elongation at break of 150.65±31.00 represents a high elastic material, consistently with the properties of PCL. The elasticity modulus obtained might vary from other reported values due to the different morphology of single fibers as most of the literature had not to report values of beaded-fibers. We speculate that beads behave in a similar way that agglomerates and can act as stress raisers, that avoid the distribution of stress[62]. It finally reflects in a detriment of some of the mechanical properties of the beads-on-string membrane in comparison to the regularly reported non-beaded

A)

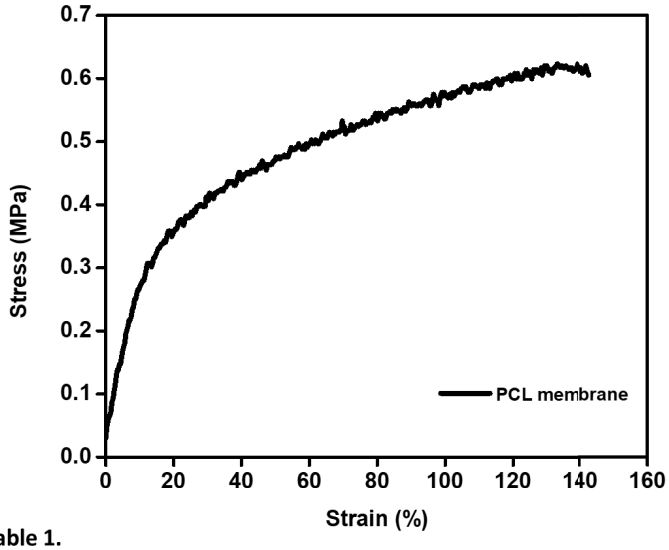

B) Table 1.

Sample	Young's modulus (MPa)	Yield Strength (MPa)	Ultimate tensile strength (MPa)	Fracture point (MPa)	Elongation at break (%)
PCL	2.29 ± 0.13	0.22 ± 0.08	0.54 ± 0.07	0.52 ± 0.08	150.65 ± 31.00

Figure 3. Mechanical testing of PCL membrane **A)** Stress-strain curve of electrospun PCL beads-on-string membrane **B)** Table 1. Tensile properties of electrospun PCL beads-on-string membrane.

fibers. However, the PCL beaded membrane remains a high elasticity modulus and topographical characteristics to be considered a promissory scaffold.

3.2. Response of hFOB cells to micro and nanotopography

3.2.1. Cell adhesion and morphology

We have designed beaded PCL membranes with increased surface area, which can provide suitable anchorage points for cell adhesion. The prepared membranes show beaded nanofibers that are interconnected while providing void spaces that would allow cell growth. After membrane fabrication, hFOB cells were pipetted and seeded on each beaded membranes as can be noted from **Figure 4 and Supporting Information Figure S4** filopodia were extended from the osteoblast surface on to the surface of beads and used as anchorage points. On the other hand, SEM micrographs reveal the formation of mineralization nodules on the outer periphery of the cell surface was observed after 2, 7 and 14 days of cell culture while showing an extended, flattened cell morphology (**Figure 5**). As further evidence on the suitability of the beads-on-string membranes to allow proper cell maturation, labeling of the actin cytoskeleton with Phalloidin-TRITC was performed.

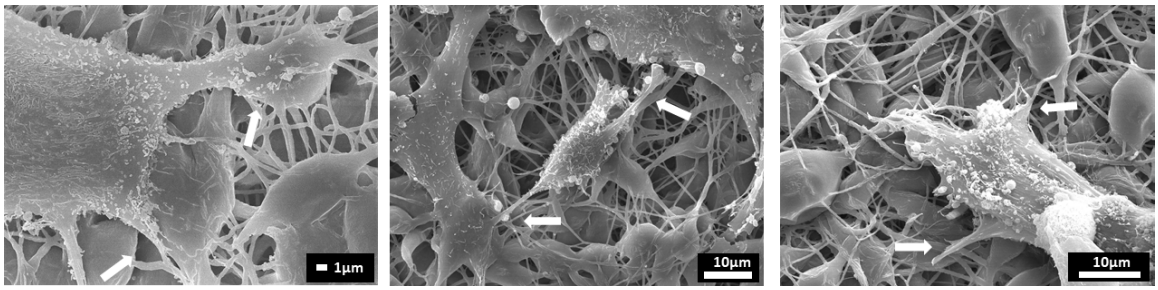

Figure 4. SEM micrographs of the hFOB cells attached to the PCL beads-on-string scaffold membrane. Interaction between cell filopodia (white arrows) and the beaded substrate can be appreciated, as well as the presence of mineralization nodules on the top of the cell's membrane. These SEM images were taken after 2 days of culture.

The results of these experiments reveal elongated and polygonal cell morphology that extends throughout the beaded substrate **(Figure 5).** It should be noted that this process of cell adhesion is an important event that determines early on other important cell activities such as proliferation and subsequent differentiation [63]. Likewise, cell-cell contact and confluence are fundamentally important for osteoblast development as it provides cells with direct signaling stimulation that can further direct the process of cell maturation and differentiation [64](**Supporting Information Figure S5).** Material surface topography and morphology has been known to affect the overall properties of cellular adhesion [65-68]. A study by Faia-Torres et al. demonstrated the effects of surface roughness in promoting osteogenic markers for hBM-mesenchymal stem cells (MSCs) by growing them on PCL roughness gradient membranes. The researchers found that regarding cytoskeletal morphology, matrix mineralization and the degree of alkaline phosphatase (ALP) and type I collagen expression was enhanced by increased surface roughness [64]. To this extent, osteoblast cell morphology and spreading on the beaded scaffolds were also observed at different time intervals (7 and 14 days).

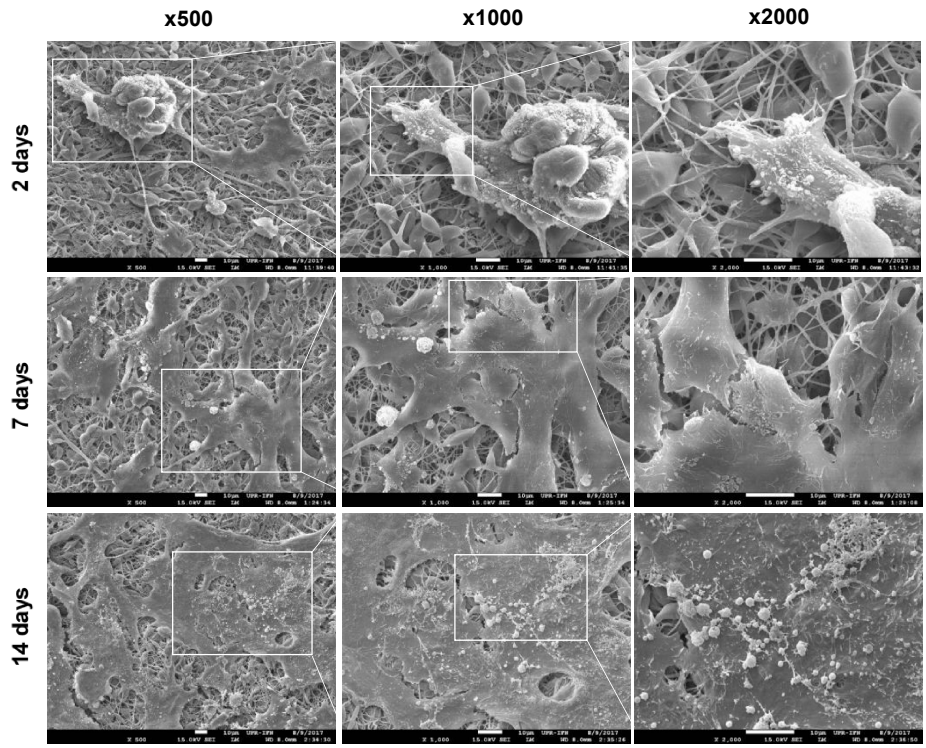

Figure 5. Scanning electron micrograph of osteoblast cultured on PCL beaded-membrane at different time intervals. Cells show proper adhesion and extended morphology as well good interconnectivity along the beaded surface. The presence of mineralization particles can be well appreciated throughout the different time's intervals but is particularly noticeable at the 14 days mark. Scale bar = 10 µm.

3.2.2 Cell proliferation

In the interest of studying how the beaded nanofibers affect the proliferation, osteoblast cells cultured on the scaffolds for 48 hours were subsequently incubated with supplemented medium containing bromodeoxyuridine (BrdU) for an additional 6 hours. This thymidine analog is incorporated into DNA during cell division and serves as a method for analyzing relative proliferation levels. Likewise, DAPI, which binds to the minor groove of DNA, was used as a counterstain to mark cell nuclei (**Figure. 6a**). As can be observed from **Figure 6b**, the percentage of cells that incorporated BrdU show no statistical differences between cultures on the beaded and the control groups. Such results allow us to assess that the presence of beaded fibers is not detrimental nor significantly affect cell proliferation.

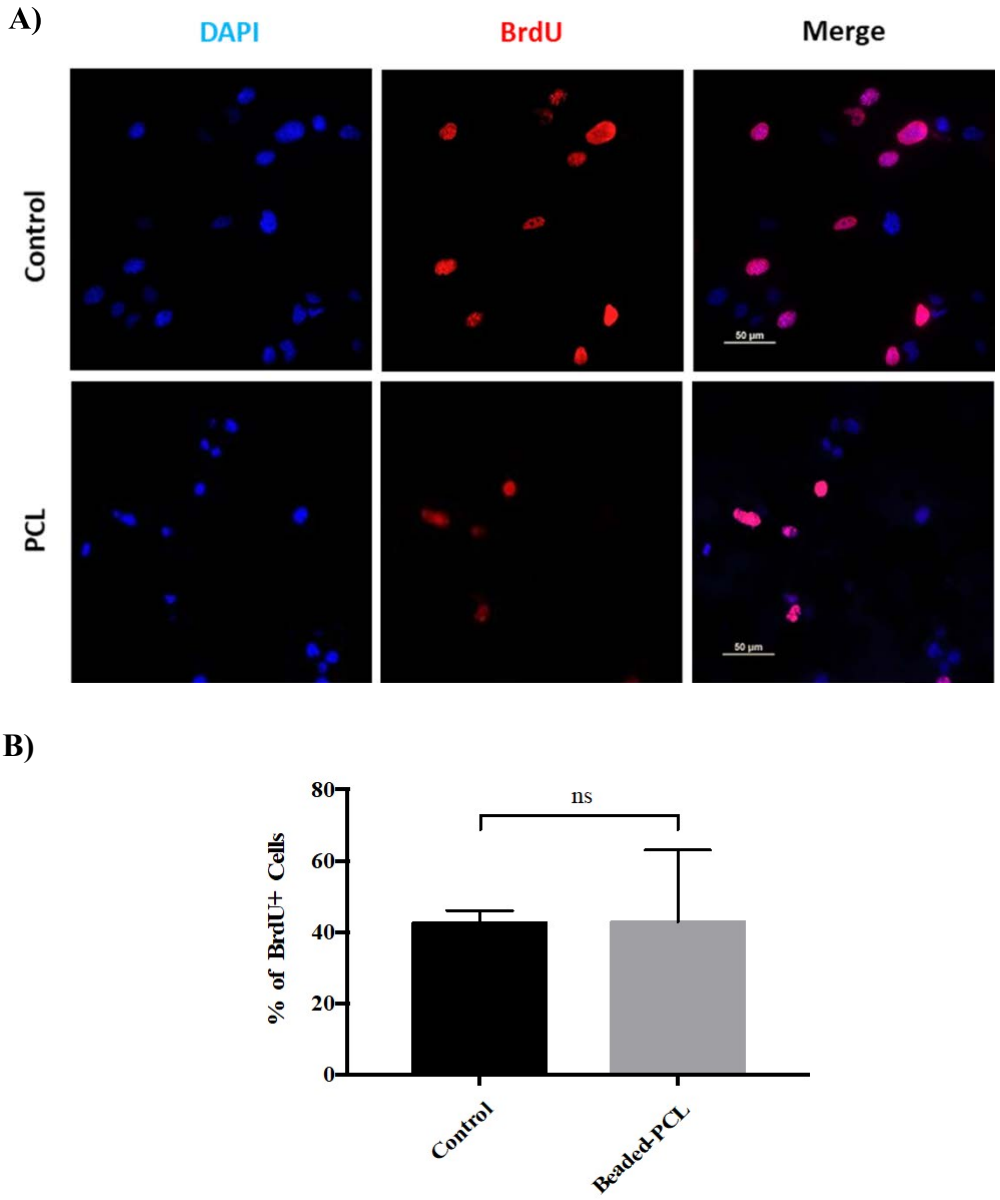

Figure 6. A) Fluorescent images showing hFOB cell proliferation on beaded scaffolds and control after 48 hours of cell culture. **B)** Statistical t-test analysis of BrdU-positive cells on control and beaded PCL substrate. Each bar represents the mean percentage of BrdU-positive nuclei ± S.D. counted in at least 2 visual fields at 40X. Scale bar = 50 µm

3.2.3 Cell Differentiation

On the other hand, hFOB cells differentiation results in the formation of mature cells that express proteins that supports the mineralization of the ECM. One of the most relevant of these expressed proteins is that of bone sialoprotein (BSP). According to Gordon et al., BSP is expressed in abundance by osteoblast cells, which shows to have a key role in the development of the mineralized tissue and help influence the process of differentiation [69]. In this regard, we have studied the expression of BSP at 7 and 14 days of cell growth. As shown in **Figure 7**, there is an abundant presence of cells expressing the matrix protein as well as the formation of cell aggregates at 7 days of culture. Nevertheless, at 14 days the cells shown to be even more prominent with an equal degree of BSP expression and good distribution throughout the material substrate. In all, these results allow us to confirm that beaded fibers provide good surface topography for cell proliferation and growth.

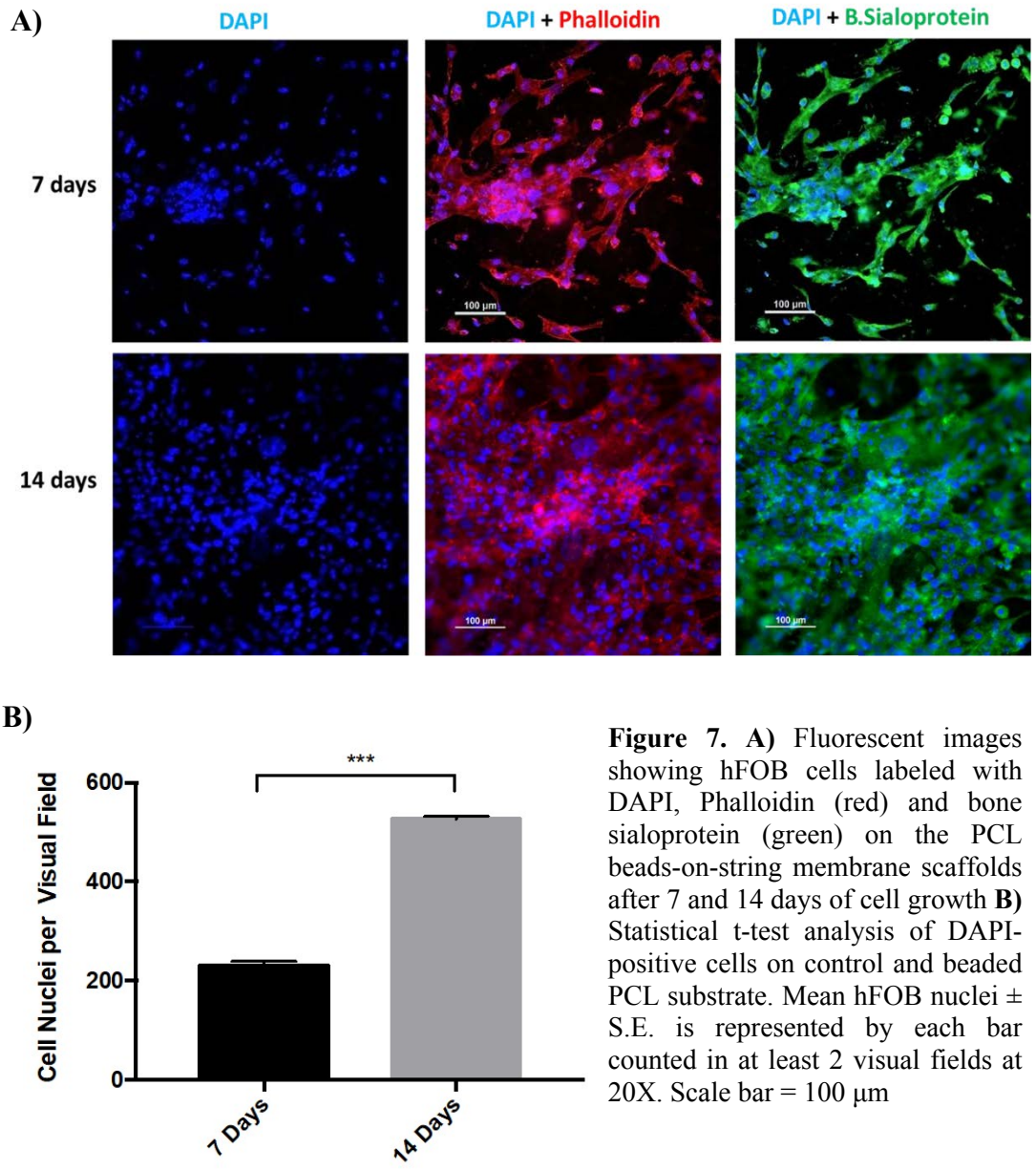

Figure 7. A) Fluorescent images showing hFOB cells labeled with DAPI, Phalloidin (red) and bone sialoprotein (green) on the PCL beads-on-string membrane scaffolds after 7 and 14 days of cell growth **B)** Statistical t-test analysis of DAPI-positive cells on control and beaded PCL substrate. Mean hFOB nuclei ± S.E. is represented by each bar counted in at least 2 visual fields at 20X. Scale bar = 100 µm

4. CONCLUSIONS

In summary, beads-on-string scaffolds were successfully prepared by adjusting and optimizing the electrospinning parameters in a systematic process. This work demonstrates the positive influence of beads-on-string, micro, and nanotopography, on the regulation of cell functions. SEM characterization confirmed the formation of microbeads and nanofibers on the

scaffolds and also showed how beads worked as anchorage points for osteoblasts filopodia. Since at the first 2 days, cells attached on scaffold had low proliferation, after 7 and 14 days of culture, osteoblasts achieve enough confluence and maturation to secrete bone sialoprotein, a significant glycoprotein expressed in mineralized tissues. Our results indicate that PCL beads-on-string scaffolds are a promising scaffold for bone tissue regeneration because it promotes osteoblast adhesion, subsequently proliferation, and differentiation.

ASSOCIATED CONTENT

Supporting Information

The design matrix of the beads-on-string experiment at different electrospinning parameters and PCL concentrations. SEM images with all the possible combinations of the high and low level of the electrospinning parameters. SEM images showing the bump-like structure of the PCL nanofibers. FTIR spectra and XRD diffractogram of PCL. SEM images showing osteoblasts attachment in the beads-on-string scaffolds. SEM images showing the confluence of osteoblasts on the scaffolds.

ACKNOWLEDGEMENTS

The authors acknowledge the support and resources of the University of Puerto Rico (UPR), The Molecular Science Research Center (MSRC) and the Material Characterization Center (MCC). This work was funded by the Research Initiative for Scientific Enhancement (RISE) Program Grant 5R25GM061151-15 and the PR NASA Space Grant NNX15AI11H. This work was partly supported by NASA Experimental Program to Stimulate Competitive Research (EPSCoR) grant NNX14AN18A and for NSF REU: PR Climb Program Grant 1560278. The authors thank the facility support of the Neuroimaging and Electrophysiology Facility Grant NIH P20GM103642.

Finally, we are very grateful to Dr. José E. García-Arrarás of the University of Puerto Rico, Río Piedras campus for allowing the use of the Fluorescence Microscope obtained under grant NSF IOS-1252679.

,

AUTHORS INFORMATION

Corresponding Author, * Prof. Eduardo Nicolau, eduardo.nicolau@upr.edu

Present Addresses

(E.N.) Department of Chemistry, University of Puerto Rico, Rio Piedras Campus, 17 Ave. Universidad Ste. 1701, San Juan, Puerto Rico USA 00925-2537// Molecular Science Research Center, University of Puerto Rico, 1390 Ponce De Leon Ave, Suite 2, San Juan Puerto Rico USA 00931-3346

Jaime Santillán, jaime.santillan@upr.edu

Emmanuel A. Dwomoh, kofidwomoh20@gmail.com

Yaiel G. Rodríguez-Avilés, yaiel.rodriguez@upr.edu

Samir A. Bello, samir.bello@upr.edu

Author Contributions

The manuscript was written through the contributions of all authors. All authors have given approval to the final version of the manuscript.

REFERENCES

1. Frantz, C.; Stewart, K. M.; Weaver, V. M., The Extracellular Matrix at a Glance. *J. Cell Sci.* **2010,** *123* (Pt 24), 4195-4200. DOI: 10.1242/jcs.023820.
2. Gattazzo, F.; Urciuolo, A.; Bonaldo, P., Extracellular Matrix: A Dynamic Microenvironment for Stem Cell Niche. *Biochim. Biophys. Acta* **2014,** *1840* (8), 2506-2519. DOI: 10.1016/j.bbagen.2014.01.010.
3. Sampath, T. K., Importance of Geometry of the Extracellular Matrix in Endochondral Bone Differentiation. *J. Cell Biol.* **1984,** *98* (6), 2192-2197. DOI: 10.1083/jcb.98.6.2192.
4. Danie Kingsley, J.; Ranjan, S.; Dasgupta, N.; Saha, P., Nanotechnology for Tissue Engineering: Need, Techniques And applications. *J. Pharm. Res.* **2013,** *7* (2), 200-204. DOI: 10.1016/j.jopr.2013.02.021.
5. Czeisler, C.; Short, A.; Nelson, T.; Gygli, P.; Ortiz, C.; Catacutan, F. P.; Stocker, B.; Cronin, J.; Lannutti, J.; Winter, J.; Otero, J. J., Surface Topography During Neural Stem Cell Differentiation Regulates Cell Migration and Cell Morphology. *J. Comp. Neurol.* **2016,** *524* (17), 3485-3502. DOI: 10.1002/cne.24078.
6. Chrischilles, E. A.; Butler, D. C.; Davis, C. S.; Wallace, R. B., A Model of Lifetime Osteoporosis Impact. *Arch. Intern. Med.* **1991,** *151* (10), 2026-2032. DOI: 10.1001/archinte.1991.00400100100017.
7. Shi, C.; Yuan, Z.; Han, F.; Zhu, C.; Li, B., Polymeric Biomaterials for Bone Regeneration. *Ann. Joint* **2016,** *1*, 27-27. DOI: 10.21037/aoj.2016.11.02.
8. Gong, T.; Xie, J.; Liao, J.; Zhang, T.; Lin, S.; Lin, Y., Nanomaterials and Bone Regeneration. *Bone Res.* **2015,** *3*, 15029. DOI: 10.1038/boneres.2015.29.
9. Chen, E.; Yang, L.; Ye, C.; Zhang, W.; Ran, J.; Xue, D.; Wang, Z.; Pan, Z.; Hu, Q., An Asymmetric Chitosan Scaffold for Tendon Tissue Engineering: In Vitro and in Vivo Evaluation with Rat Tendon Stem/Progenitor Cells. *Acta Biomater.* **2018,** *73*, 377-387. DOI: 10.1016/j.actbio.2018.04.027.
10. Ratcliffe, A.; Butler, D. L.; Dyment, N. A.; Cagle, P. J., Jr.; Proctor, C. S.; Ratcliffe, S. S.; Flatow, E. L., Scaffolds for Tendon and Ligament Repair and Regeneration. *Ann. Biomed. Eng.* **2015,** *43* (3), 819-831. DOI: 10.1007/s10439-015-1263-1.
11. Kerativitayanan, P.; Tatullo, M.; Khariton, M.; Joshi, P.; Perniconi, B.; Gaharwar, A. K., Nanoengineered Osteoinductive and Elastomeric Scaffolds for Bone Tissue Engineering. *ACS Biomater. Sci. Eng.* **2017,** *3* (4), 590-600. DOI: 10.1021/acsbiomaterials.7b00029.
12. Diban, N.; Stamatialis, D. F., Functional Polymer Scaffolds for Blood Vessel Tissue Engineering. *Macromol. Symp.* **2011,** *309-310* (1), 93-99. DOI: 10.1002/masy.201100038.
13. Li, X.; Wang, L.; Fan, Y.; Feng, Q.; Cui, F. Z.; Watari, F., Nanostructured Scaffolds for Bone Tissue Engineering. *J. Biomed. Mater. Res., Part A* **2013,** *101* (8), 2424-2435. DOI: 10.1002/jbm.a.34539.
14. Bancelin, S.; Aime, C.; Gusachenko, I.; Kowalczuk, L.; Latour, G.; Coradin, T.; Schanne-Klein, M. C., Determination of Collagen Fibril Size Via Absolute Measurements of Second-Harmonic Generation Signals. *Nat. Commun.* **2014,** *5*, 4920. DOI: 10.1038/ncomms5920.
15. Buehler, M. J., Nature Designs Tough Collagen: Explaining the Nanostructure of Collagen Fibrils. *Proc. Natl. Acad. Sci. U. S. A.* **2006,** *103* (33), 12285-12290. DOI: 10.1073/pnas.0603216103.
16. Harvey, A. G.; Hill, E. W.; Bayat, A., Designing Implant Surface Topography for Improved Biocompatibility. *Expert Rev. Med. Devices* **2013,** *10* (2), 257-267. DOI: 10.1586/erd.12.82.
17. Yoo, H. S.; Kim, T. G.; Park, T. G., Surface-Functionalized Electrospun Nanofibers for Tissue Engineering and Drug Delivery. *Adv. Drug Delivery Rev.* **2009,** *61* (12), 1033-1042. DOI: 10.1016/j.addr.2009.07.007.
18. Yoshida, S.; Hagiwara, K.; Hasebe, T.; Hotta, A., Surface Modification of Polymers by Plasma Treatments for the Enhancement of Biocompatibility and Controlled Drug Release. *Surf. Coat. Technol.* **2013,** *233*, 99-107. DOI: 10.1016/j.surfcoat.2013.02.042.
19. Klee, D.; Villari, R. V.; Höcker, H.; Dekker, B.; Mittermayer, C., Surface Modification of a New Flexible Polymer with Improved Cell Adhesion. *J. Mater. Sci.: Mater. Med.* **1994,** *5* (9-10), 592-595. DOI: 10.1007/bf00120336.
20. Rajajeyaganthan, R.; Kessler, F.; de Mour Leal, P. H.; Kühn, S.; Weibel, D. E., Surface Modification of Synthetic Polymers Using Uv Photochemistry in the Presence of Reactive Vapours. *Macromol. Symp.* **2011,** *299-300* (1), 175-182. DOI: 10.1002/masy.200900128.
21. Shahabi, S.; Najafi, F.; Majdabadi, A.; Hooshmand, T.; Haghbin Nazarpak, M.; Karimi, B.; Fatemi, S. M., Effect of Gamma Irradiation on Structural and Biological Properties of a Plga-Peg-Hydroxyapatite Composite. *Sci. World J.* **2014,** *2014*, 9. DOI: 10.1155/2014/420616.

22. Huang, Q.; Elkhooly, T. A.; Liu, X.; Zhang, R.; Yang, X.; Shen, Z.; Feng, Q., Effects of Hierarchical Micro/Nano-Topographies on the Morphology, Proliferation and Differentiation of Osteoblast-Like Cells. *Colloids Surf., B* **2016,** *145*, 37-45. DOI: 10.1016/j.colsurfb.2016.04.031.
23. Kriparamanan, R.; Aswath, P.; Zhou, A.; Tang, L.; Nguyen, K. T., Nanotopography: Cellular Responses to Nanostructured Materials. *J. Nanosci. Nanotechnol.* **2006,** *6* (7), 1905-1919. DOI: 10.1166/jnn.2006.330.
24. Lyu, S.; Huang, C.; Yang, H.; Zhang, X., Electrospun Fibers as a Scaffolding Platform for Bone Tissue Repair. *J. Orthop. Res.* **2013,** *31* (9), 1382-1389. DOI: 10.1002/jor.22367.
25. Senthamizhan, A.; Balusamy, B.; Uyar, T., 1 - Electrospinning: A Versatile Processing Technology for Producing Nanofibrous Materials for Biomedical and Tissue-Engineering Applications. In *Electrospun Mater. Tissue Eng. Biomed. Appl.*, Uyar, T.; Kny, E., Eds. Woodhead Publishing: 2017; pp 3-41. DOI: 10.1016/b978-0-08-101022-8.00001-6.
26. Li, T.; Ding, X.; Tian, L.; Ramakrishna, S., Engineering Bsa-Dextran Particles Encapsulated Bead-on-String Nanofiber Scaffold for Tissue Engineering Applications. *J. Mater. Sci.* **2017,** *52* (18), 10661-10672. DOI: 10.1007/s10853-017-1245-9.
27. Li, T.; Ding, X.; Tian, L.; Hu, J.; Yang, X.; Ramakrishna, S., The Control of Beads Diameter of Bead-on-String Electrospun Nanofibers and the Corresponding Release Behaviors of Embedded Drugs. *Mater. Sci. Eng., C* **2017,** *74*, 471-477. DOI: 10.1016/j.msec.2016.12.050.
28. Fong, H.; Chun, I.; Reneker, D. H., Beaded Nanofibers Formed During Electrospinning. *Polymer* **1999,** *40* (16), 4585-4592. DOI: 10.1016/s0032-3861(99)00068-3.
29. Li, Z.; Wang, C., Effects of Working Parameters on Electrospinning. In *One-Dimensional Nanostructures: Electrospinning Technique and Unique Nanofibers*, Li, Z.; Wang, C., Eds. Springer Berlin Heidelberg: Berlin, Heidelberg, 2013; pp 15-28. DOI: 10.1007/978-3-642-36427-3_2.
30. Liu, W.; Thomopoulos, S.; Xia, Y., Electrospun Nanofibers for Regenerative Medicine. *Adv. Healthcare Mater.* **2012,** *1* (1), 10-25. DOI: 10.1002/adhm.201100021.
31. Tsai, S. W.; Chen, C. C.; Chen, P. L.; Hsu, F. Y., Influence of Topography of Nanofibrils of Three-Dimensional Collagen Gel Beads on the Phenotype, Proliferation, and Maturation of Osteoblasts. *J. Biomed. Mater. Res., Part A* **2009,** *91* (4), 985-993. DOI: 10.1002/jbm.a.32324.
32. Hong, J. K.; Bang, J. Y.; Xu, G.; Lee, J. H.; Kim, Y. J.; Lee, H. J.; Kim, H. S.; Kwon, S. M., Thickness-Controllable Electrospun Fibers Promote Tubular Structure Formation by Endothelial Progenitor Cells. *Int. J. Nanomed.* **2015,** *10*, 1189-1200. DOI: 10.2147/IJN.S73096.
33. Yu, J. H.; Fridrikh, S. V.; Rutledge, G. C., The Role of Elasticity in the Formation of Electrospun Fibers. *Polymer* **2006,** *47* (13), 4789-4797. DOI: 10.1016/j.polymer.2006.04.050.
34. Heydari, Z.; Mohebbi-Kalhori, D.; Afarani, M. S., Engineered Electrospun Polycaprolactone (Pcl)/Octacalcium Phosphate (Ocp) Scaffold for Bone Tissue Engineering. *Mater. Sci. Eng., C* **2017,** *81*, 127-132. DOI: 10.1016/j.msec.2017.07.041.
35. Ronca, D.; Langella, F.; Chierchia, M.; D'Amora, U.; Russo, T.; Domingos, M.; Gloria, A.; Bartolo, P.; Ambrosio, L., Bone Tissue Engineering: 3d Pcl-Based Nanocomposite Scaffolds with Tailored Properties. *Procedia CIRP* **2016,** *49*, 51-54. DOI: 10.1016/j.procir.2015.07.028.
36. Gorodzha, S. N.; Muslimov, A. R.; Syromotina, D. S.; Timin, A. S.; Tcvetkov, N. Y.; Lepik, K. V.; Petrova, A. V.; Surmeneva, M. A.; Gorin, D. A.; Sukhorukov, G. B.; Surmenev, R. A., A Comparison Study between Electrospun Polycaprolactone and Piezoelectric Poly(3-Hydroxybutyrate-Co-3-Hydroxyvalerate) Scaffolds for Bone Tissue Engineering. *Colloids Surf., B* **2017,** *160*, 48-59. DOI: 10.1016/j.colsurfb.2017.09.004.
37. Santoro, M.; Shah, S. R.; Walker, J. L.; Mikos, A. G., Poly(Lactic Acid) Nanofibrous Scaffolds for Tissue Engineering. *Adv. Drug Delivery Rev.* **2016,** *107*, 206-212. DOI: 10.1016/j.addr.2016.04.019.
38. Ding, Y.; Li, W.; Muller, T.; Schubert, D. W.; Boccaccini, A. R.; Yao, Q.; Roether, J. A., Electrospun Polyhydroxybutyrate/Poly(Epsilon-Caprolactone)/58s Sol-Gel Bioactive Glass Hybrid Scaffolds with Highly Improved Osteogenic Potential for Bone Tissue Engineering. *ACS Appl. Mater. Interfaces* **2016,** *8* (27), 17098-17108. DOI: 10.1021/acsami.6b03997.
39. Vainionpää, S., Biodegradation of Polyglycolic Acid in Bone Tissue: An Experimental Study on Rabbits. *Arch. Orthop. Unfall-Chir.* **1986,** *104* (6), 333-338. DOI: 10.1007/bf00454425.
40. Woodruff, M. A.; Hutmacher, D. W., The Return of a Forgotten Polymer—Polycaprolactone in the 21st Century. *Prog. Polym. Sci.* **2010,** *35* (10), 1217-1256. DOI: 10.1016/j.progpolymsci.2010.04.002.
41. Rai, A.; Senapati, S.; Saraf, S. K.; Maiti, P., Biodegradable Poly(E-Caprolactone) as a Controlled Drug Delivery Vehicle of Vancomycin for the Treatment of Mrsa Infection. *J. Mater. Chem. B* **2016,** *4* (30), 5151-5160. DOI: 10.1039/c6tb01623e.

42. Eshraghi, S.; Das, S., Mechanical and Microstructural Properties of Polycaprolactone Scaffolds with One-Dimensional, Two-Dimensional, and Three-Dimensional Orthogonally Oriented Porous Architectures Produced by Selective Laser Sintering. *Acta Biomater.* **2010,** *6* (7), 2467-2476. DOI: 10.1016/j.actbio.2010.02.002.
43. Sun, H.; Mei, L.; Song, C.; Cui, X.; Wang, P., The in Vivo Degradation, Absorption and Excretion of Pcl-Based Implant. *Biomaterials* **2006,** *27* (9), 1735-1740. DOI: 10.1016/j.biomaterials.2005.09.019.
44. Malikmammadov, E.; Tanir, T. E.; Kiziltay, A.; Hasirci, V.; Hasirci, N., Pcl and Pcl-Based Materials in Biomedical Applications. *J. Biomater. Sci., Polym. Ed.* **2018,** *29* (7-9), 863-893. DOI: 10.1080/09205063.2017.1394711.
45. Li, H.; Xu, Y.; Xu, H.; Chang, J., Electrospun Membranes: Control of the Structure and Structure Related Applications in Tissue Regeneration and Drug Delivery. *J. Mater. Chem. B* **2014,** *2* (34), 5492-5510. DOI: 10.1039/c4tb00913d.
46. Kiremitçí, M.; Pişkin, E., Cell Adhesion to the Surfaces of Polymeric Beads. *Biomater., Artif. Cells, Artif. Organs* **2009,** *18* (5), 599-603. DOI: 10.3109/10731199009117327.
47. Furukawa, K. S.; Miyauchi, S.; Suzuki, D.; Umezu, Y.; Shinjo, T.; Ushida, T.; Eguchi, M.; Tateishi, T., Bone Tissue Engineering Based on Bead–Cell Sheets Composed of Calcium Phosphate Beads and Bone Marrow Cells. *Mater. Sci. Eng., C* **2004,** *24* (3), 437-440. DOI: 10.1016/j.msec.2003.11.010.
48. Rinoldi, C.; Kijeńska, E.; Chlanda, A.; Choinska, E.; Khenoussi, N.; Tamayol, A.; Khademhosseini, A.; Swieszkowski, W., Nanobead-on-String Composites for Tendon Tissue Engineering. *J. Mater. Chem. B* **2018,** *6* (19), 3116-3127. DOI: 10.1039/C8TB00246K.
49. Zhao, H.; Chi, H., Electrospun Bead-on-String Fibers: Useless or Something of Value? In *Novel Aspects of Nanofibers*, Intech: 2018; pp 87-102. DOI: 10.5772/intechopen.74661.
50. Vega-Figueroa, K.; Santillán, J.; García, C.; González-Feliciano, J. A.; Bello, S. A.; Rodríguez, Y. G.; Ortiz-Quiles, E.; Nicolau, E., Assessing the Suitability of Cellulose-Nanodiamond Composite as a Multifunctional Biointerface Material for Bone Tissue Regeneration. *ACS Biomaterials Science & Engineering* **2017,** *3* (6), 960-968. DOI: 10.1021/acsbiomaterials.7b00026.
51. Gokalp, N.; Ulker, C.; Guvenilir, Y. A., Synthesis of Polycaprolactone Via Ring Opening Polymerization Catalyzed by Candida Antarctica Lipase B Immobilized onto an Amorphous Silica Support. *J. Polym. Mater.* **2016,** *33* (1), 87-100.
52. Yao, Y.; Wei, H.; Wang, J.; Lu, H.; Leng, J.; Hui, D., Fabrication of Hybrid Membrane of Electrospun Polycaprolactone and Polyethylene Oxide with Shape Memory Property. *Composites, Part B* **2015,** *83*, 264-269. DOI: 10.1016/j.compositesb.2015.08.060.
53. Benkaddour, A.; Jradi, K.; Robert, S.; Daneault, C., Grafting of Polycaprolactone on Oxidized Nanocelluloses by Click Chemistry. *Nanomaterials* **2013,** *3* (1), 141-157. DOI: 10.3390/nano3010141.
54. Xue, J.; He, M.; Liang, Y.; Crawford, A.; Coates, P.; Chen, D.; Shi, R.; Zhang, L., Fabrication and Evaluation of Electrospun Pcl–Gelatin Micro-/Nanofiber Membranes for Anti-Infective Gtr Implants. *J. Mater. Chem. B* **2014,** *2* (39), 6867-6877. DOI: 10.1039/c4tb00737a.
55. Borjigin, M.; Eskridge, C.; Niamat, R.; Strouse, B.; Bialk, P.; Kmiec, E. B., Electrospun Fiber Membranes Enable Proliferation of Genetically Modified Cells. *Int. J. Nanomed.* **2013,** *8*, 855-864. DOI: 10.2147/IJN.S40117.
56. Patrício, T.; Domingos, M.; Gloria, A.; Bártolo, P., Characterisation of Pcl and Pcl/Pla Scaffolds for Tissue Engineering. *Procedia CIRP* **2013,** *5*, 110-114. DOI: 10.1016/j.procir.2013.01.022.
57. Sousa, I.; Mendes, A.; Bártolo, P. J., Pcl Scaffolds with Collagen Bioactivator for Applications in Tissue Engineering. *Procedia Eng.* **2013,** *59* (Supplement C), 279-284. DOI: 10.1016/j.proeng.2013.05.122.
58. Jenkins, M. J.; Harrison, K. L., The Effect of Crystalline Morphology on the Degradation of Polycaprolactone in a Solution of Phosphate Buffer and Lipase. *Polym. Adv. Technol.* **2008,** *19* (12), 1901-1906. DOI: 10.1002/pat.1227.
59. Qian, Y.; Zhang, Z.; Zheng, L.; Song, R.; Zhao, Y., Fabrication and Characterization of Electrospun Polycaprolactone Blended with Chitosan-Gelatin Complex Nanofibrous Mats. *J. Nanomater.* **2014,** *2014*, 1-7. DOI: 10.1155/2014/964621.
60. Gautam, S.; Chou, C.-F.; Dinda, A. K.; Potdar, P. D.; Mishra, N. C., Fabrication and Characterization of Pcl/Gelatin/Chitosan Ternary Nanofibrous Composite Scaffold for Tissue Engineering Applications. *J. Mater. Sci.* **2013,** *49* (3), 1076-1089. DOI: 10.1007/s10853-013-7785-8.
61. Augustine, R.; Nethi, S. K.; Kalarikkal, N.; Thomas, S.; Patra, C. R., Electrospun Polycaprolactone (Pcl) Scaffolds Embedded with Europium Hydroxide Nanorods (Ehns) with Enhanced Vascularization and Cell Proliferation for Tissue Engineering Applications. *J. Mater. Chem. B* **2017,** *5* (24), 4660-4672. DOI: 10.1039/c7tb00518k.

62. Augustine, R.; Malik, H. N.; Singhal, D. K.; Mukherjee, A.; Malakar, D.; Kalarikkal, N.; Thomas, S., Electrospun Polycaprolactone/Zno Nanocomposite Membranes as Biomaterials with Antibacterial and Cell Adhesion Properties. *J. Polym. Res.* **2014,** *21* (3). DOI: 10.1007/s10965-013-0347-6.
63. Anselme, K., Osteoblast Adhesion on Biomaterials. *Biomaterials* **2000,** *21* (7), 667-681. DOI: 10.1016/s0142-9612(99)00242-2.
64. Faia-Torres, A. B.; Guimond-Lischer, S.; Rottmar, M.; Charnley, M.; Goren, T.; Maniura-Weber, K.; Spencer, N. D.; Reis, R. L.; Textor, M.; Neves, N. M., Differential Regulation of Osteogenic Differentiation of Stem Cells on Surface Roughness Gradients. *Biomaterials* **2014,** *35* (33), 9023-9032. DOI: 10.1016/j.biomaterials.2014.07.015.
65. Neamnark, A.; Sanchavanakit, N.; Pavasant, P.; Rujiravanit, R.; Supaphol, P., In Vitro Biocompatibility of Electrospun Hexanoyl Chitosan Fibrous Scaffolds Towards Human Keratinocytes and Fibroblasts. *Euro. Polym. J.* **2008,** *44* (7), 2060-2067. DOI: 10.1016/j.eurpolymj.2008.04.016.
66. Ghanavati, Z.; Neisi, N.; Bayati, V.; Makvandi, M., The Influence of Substrate Topography and Biomaterial Substance on Skin Wound Healing. *Anat. Cell Biol.* **2015,** *48* (4), 251-257. DOI: 10.5115/acb.2015.48.4.251.
67. Zhao, L.; Hu, Y.; Xu, D.; Cai, K., Surface Functionalization of Titanium Substrates with Chitosan-Lauric Acid Conjugate to Enhance Osteoblasts Functions and Inhibit Bacteria Adhesion. *Colloids Surf., B* **2014,** *119*, 115-125. DOI: 10.1016/j.colsurfb.2014.05.002.
68. Kulangara, K.; Leong, K. W., Substrate Topography Shapes Cell Function. *Soft Matter* **2009,** *5* (21), 4072-4076. DOI: 10.1039/b910132m.
69. Gordon, J. A.; Tye, C. E.; Sampaio, A. V.; Underhill, T. M.; Hunter, G. K.; Goldberg, H. A., Bone Sialoprotein Expression Enhances Osteoblast Differentiation and Matrix Mineralization in Vitro. *Bone* **2007,** *41* (3), 462-473. DOI: 10.1016/j.bone.2007.04.191.

Graphical Abstract